



DOI: doi.org/10.21009/SPEKTRA.063.01

SPECTROSCOPIC AND RADIATIVE PROPERTIES OF Sm^{3+} DOPED SODIUM-LEAD-ZINC-LITHIUM-BORATE GLASSES

Donna Rajagukguk¹, Juniastel Rajagukguk^{2*}, Pintor Simamora²,
Rappel Situmorang², Chayani Sarumaha^{3,4}, Widyaningrum Indrasari⁵

¹Physics Study Program of Postgraduate School of Universitas Negeri Medan, Medan 20221, Indonesia

²Department of Physics, Faculty of Mathematics and Natural Sciences, Universitas Negeri Medan, 20221, Indonesia

³Center of Excellence in Glass Technology and Materials Science, Nakhon Pathom Rajabhat University, Nakhon Pathom, 73000, Thailand

⁴Physics Program, Faculty of Science and Technology, Nakhon Pathom Rajabhat University, 73000, Thailand

⁵Physics Department, Faculty of Mathematics and Science, Universitas Negeri Jakarta, Jakarta 13220, Indonesia

*Corresponding Author Email: juniastel@unimed.ac.id

Received: 17 October 2021
Revised: 21 November 2021
Accepted: 22 December 2021
Online: 28 December 2021
Published: 30 December 2021

SPEKTRA: Jurnal Fisika dan Aplikasinya
p-ISSN: 2541-3384
e-ISSN: 2541-3392



ABSTRACT

The glasses with a composition of $(65 - x) \text{B}_2\text{O}_3 - 5\text{ZnO} - 5\text{Li}_2\text{O} - 15 \text{Na}_2\text{O} - 10\text{PbO} - x \text{Sm}_2\text{O}_3$ ($x = 0.0; 0.05; 0.1; 0.5; 1.0; 2.0$ and 4.0 mol.%) which has been prepared using the melt quenching technique (1100°C for 3 hour). The spectroscopic properties can be determined by investigating the absorption, excitation, and emission spectra of a glass sample. There are 14 centered absorption bands starting from $^6\text{H}_{5/2}$. The excitation spectrum of the Sm^{3+} doped borate glasses was measured at the wavelength of 300-550 nm which is the strongest intensity ($^4\text{F}_{7/2}$ at 403 nm) used as the excitation wavelength to measure the glass emission spectrum. The emission peaks transition starts from $^4\text{G}_{5/2}$. The Judd-Ofelt theory has been applied to the absorption spectrum of Sm^{3+} doped borate glass to estimate the intensity parameters (Ω_λ , $\lambda = 2, 4$ and 6) which are then used to calculate the radiative properties. The energy of the optical bandgap is in the range 3.85-3.77 eV for direct transitions and 3.42 - 4.22 eV for indirect transitions. The decay times obtained were 3.42, 3.99, 3.98, 2.96, 1.67, 1.48 ms for 0.05 - 4.00 mol%. Using the CIE chromaticity diagram for borate glass it can be determined that the

glass from this work has a high performance for use as an orange emitting material application.

Keywords: radiative, spectroscopic, borate glass

INTRODUCTION

Many researchers have paid great attention to research on rare-earth ions, in particular for the material of glass. A glass doped with rare earth ions is an important material in the manufacture of lasers, laser waveguides, and fiber optics [1-4]. It causes rare-earth ions can emit visible light, near-infrared (NIR), and infrared (infrared), and rare earth ions to have very stable emissions due to the 4f-4f electronic transition [5-6].

For all of the rare earth ions, Samarium (Sm^{3+}) is one of the most attractive rare-earth ions for use as fluorescent in the orange region (${}^4\text{G}_{5/2} \rightarrow {}^6\text{H}_{7/2}$) [7]. In addition, Sm^{3+} doped glass has been considered a promising luminescence material for the device's appearance and orange emitting material [7-8]. This is in line with previous research which stated that Sm^{3+} is one of the rare-earth ions used as a luminescence material such as high density optical storage, different color rendition of fluorescent devices and solid state lasers as a result of a strong orange/red light emitting [2, 9].

The performance of rare-earth doped glass is highly dependent on the host-glass composition and the rare-earth dopant ion concentration [10]. Borate (B_2O_3) is one of the best glass formers known for its unprecedented features such as high transparency, low melting point, high chemical resistance, low production costs, and high thermal resistance [11-12]. On the other hand, however, borate glass has one disadvantage, which is that it has high phonon energy (1300 cm^{-1}) and produces multi-phononic relaxation for rare-earth ions, which results in non-radiation emission [13]. To suppress excess phonon energy and thereby increase the radiation emission capacity of the main material, a suitable metal such as PbO can be added to the borate [14]. The presence of lead ions (Pb^{2+}) will provide a huge advantage in the spectroscopic characterization of the RE ion. There is also a strong absorption in the UV region due to the electronic transition of S-P from the Pb^{2+} ion [15]. Sodium oxide (Na_2O) added to borate glass makes this glass suitable for use as a luminescent material for optical applications, especially because of its good solubility of rare-earth ions [11]. Then to increase the density and refractive index added ZnO and the addition of Li_2O for a high degree of transparency and thermal equilibrium in the borate glass [2, 16].

We report the results in this study, among others, optical properties, luminescence properties, and radiative properties of borate glass doped with Samarium (Sm^{3+}). Judd-Ofelt parameter analysis is used to obtain radiation rate, branching ratio, lifetime, emission cross-section by first obtaining absorption and emission spectra measurements.

METHOD

In this study, the glass developed was borate-type glass with a glass medium added with rare earth ion doping. Chemical formulations developed is $(65 - x)\text{B}_2\text{O}_3 - 5\text{ZnO} - 5\text{Li}_2\text{O} - 15\text{Na}_2\text{O} - 10\text{PbO} - x\text{Sm}_2\text{O}_3$ (where $x = 0.05; 0.1; 0.5; 1.0; 2.0$ and $4.0\text{ mol}\%$) with sample code were

BZLNPSm 0.05; BZLNPSm 0.1; BZLNPSm 0.5; BZLNPSm 1.0; BZLNPSm 2.0; BZLNPSm 4.0 respectively. The high purity chemical with a total mass of 20 g is prepared by the melt quenching technique. The composition mixture is placed in an alumina crucible for processing melt-quenched in a furnace at a temperature of 1100°C for 3 hours. Samples were also annealed at 500°C for 3 hours. After the previously heated mixture is cooled and the sample is produced in the form of a glass solid, then a cutting process is carried out with dimensions of 20 x 10 x 5 mm³ and polish.

After the sample is cut and polished, the synthesis process is carried out using a spectrophotometer to determine spectroscopic properties (absorption, excitation, emissions, etc) and using JO parameters to get radiative properties (branching ratio, lifetime, emission cross-section).

RESULT AND DISCUSSION

Absorption Properties

FIGURE 1 shows the absorbance spectrum of Sm³⁺ doped borate glass. It can be seen in FIGURE 1 that there are 14 centered absorption bands at 341, 362, 377, 403, 439, 475, 947, 1080, 1234, 1376, 1476, 1520, 1583, 2022 nm corresponding to the transitions from ⁶H_{5/2} to ⁴D_{7/2}, ⁴D_{3/2}, ⁴D_{1/2}, ⁴F_{7/2}, ⁴G_{9/2}, ⁴I_{11/2}, ⁶F_{11/2}, ⁶F_{9/2}, ⁶F_{7/2}, ⁶F_{5/2}, ⁶F_{3/2}, ⁶H_{15/2}, ⁶F_{1/2}, ⁶H_{13/2}. The most striking Sm₂O₃ ion absorption is 403 and 1234 nm in the Vis and NIR regions and the intensity of the absorption band is directly proportional to the concentration of rare earth ions where the absorption band increases with increasing Sm₂O₃ concentration [6, 17-20].

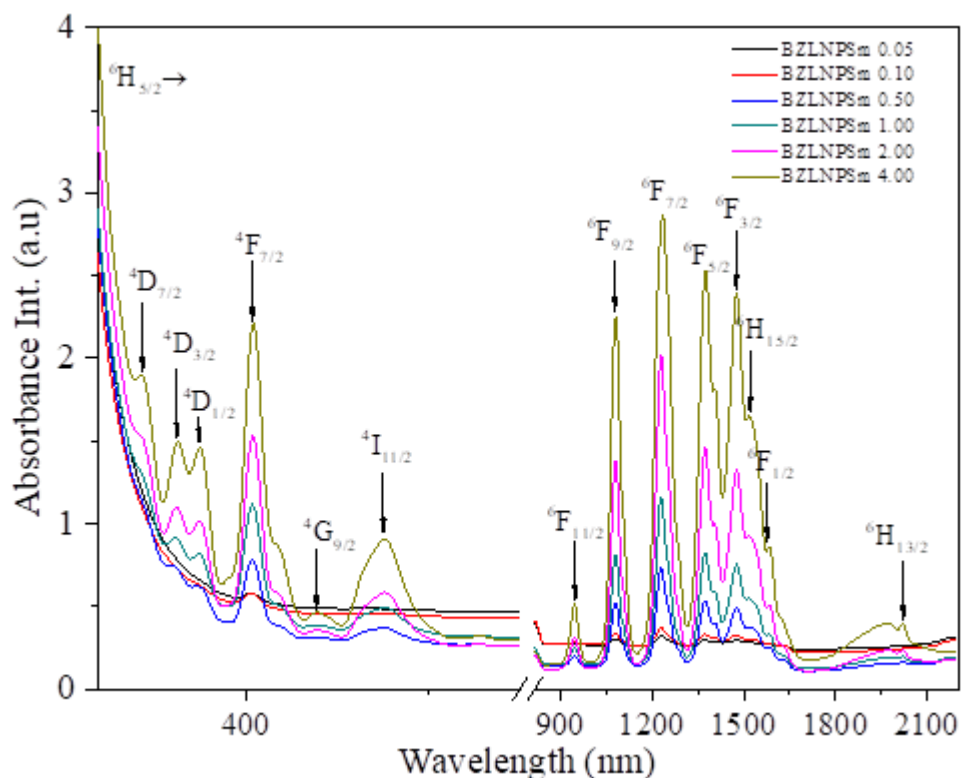


FIGURE 1. Absorption spectra of Sm³⁺ doped borate glasses.

Emission Spectra

FIGURE 2 shows the excitation spectrum of the Sm^{3+} doped borate glasses measured at the wavelength of 300-550 nm monitored at 599 nm emission. Excitation bands centered on 318, 345, 362, 375, 403, 416, 439, 463, 477, 527 nm, corresponds to ${}^6\text{H}_{5/2}$ to ${}^4\text{F}_{11/2}$, ${}^3\text{D}_{7/2}$, ${}^4\text{D}_{3/2}$, ${}^4\text{D}_{1/2}$, ${}^4\text{F}_{7/2}$, ${}^6\text{P}_{5/2}$; ${}^4\text{M}_{19/2}$, ${}^4\text{G}_{9/2}$; ${}^4\text{I}_{15/2}$, ${}^4\text{I}_{13/2}$, ${}^4\text{I}_{11/2}$; ${}^4\text{M}_{15/2}$ and ${}^4\text{F}_{3/2}$ respectively. For all of the excitation transitions, the excitation peak ${}^6\text{H}_{5/2}$ to ${}^4\text{F}_{7/2}$ at 403 nm represents the strongest intensity used as the excitation wavelength to measure the glass emission spectrum [20-21]. The emission spectrum from the glass system measured under excitation 403 nm in the 525-700 nm wavelength region is presented in FIGURE 3. The emission peaks at 563, 599, and 645 correspond to the transition ${}^4\text{G}_{5/2}$ to ${}^6\text{H}_{5/2}$, ${}^6\text{H}_{7/2}$ and ${}^6\text{H}_{9/2}$ respectively. Among the three transitions the most intense were ${}^4\text{G}_{5/2}$ to ${}^6\text{H}_{7/2}$, which emitted orange fluorescence, while the weakest ${}^6\text{G}_{5/2}$ to ${}^6\text{H}_{5/2}$ indicated red emission [21-22]. It can be observed from FIGURE 3 that the peak intensity increases, namely the increase in Sm_2O_3 content up to 1 mol% and then decreases [23]. So the optimum concentration of Sm_2O_3 in a borate glass is 1 mol% which results in the highest intensity coming out of the glass sample [6]. Then in FIGURE 4 shows a diagram of the energy level of the Sm^{3+} ion in a borate glass. Emission transitions corresponding to ${}^4\text{G}_{5/2}$ to ${}^6\text{H}_{5/2}$, ${}^6\text{H}_{7/2}$, ${}^6\text{H}_{9/2}$ resulted from rapid non-radiative multiphonon (NR) relaxation from the excited state to the ${}^4\text{G}_{5/2}$ level. In addition, the emission band from the ${}^4\text{F}_{3/2}$ level to the ${}^6\text{P}_{5/2}$; ${}^4\text{M}_{19/2}$ level is negligible compared to the emission from the ${}^4\text{G}_{5/2}$ level due to the high energy phonons in the glass material [2].

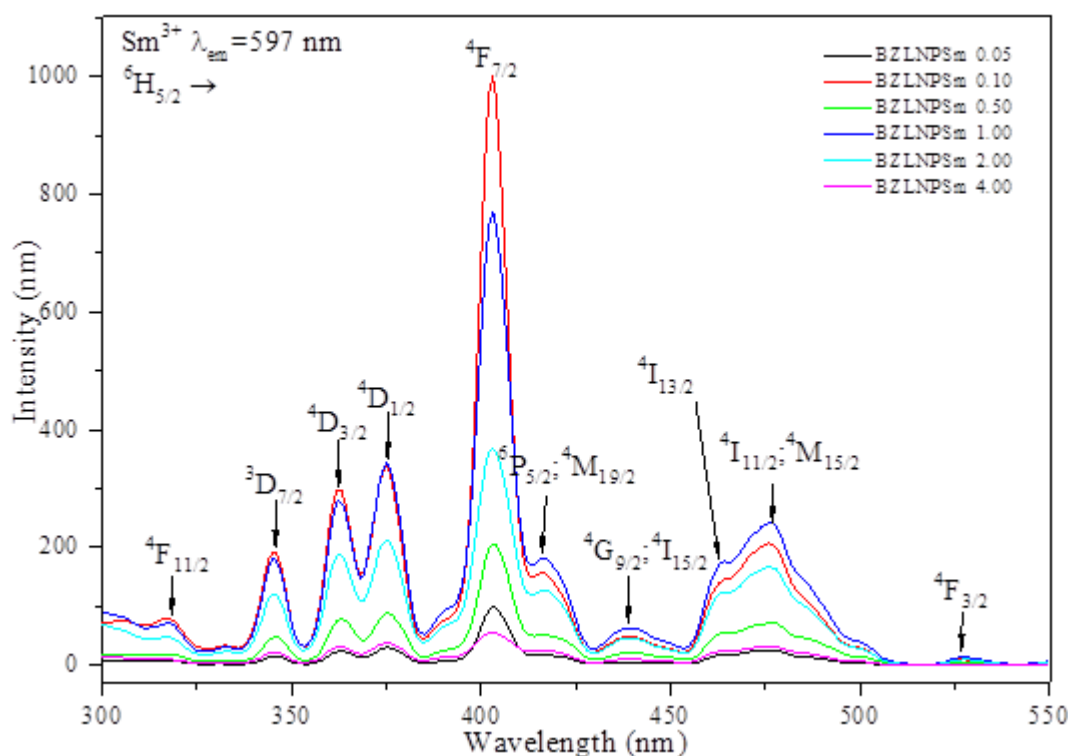


FIGURE 2. Excitation spectrum of Sm^{3+} doped borate glass.

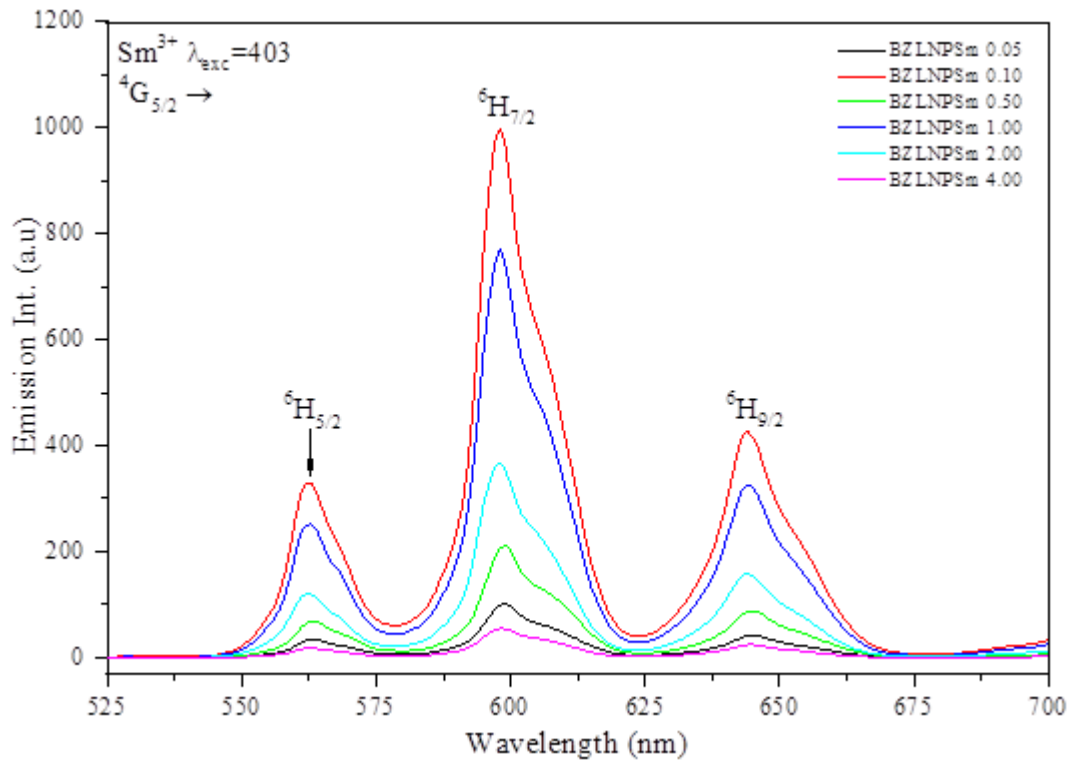


FIGURE 3. Emission spectrum of Sm^{3+} doped borate glass.

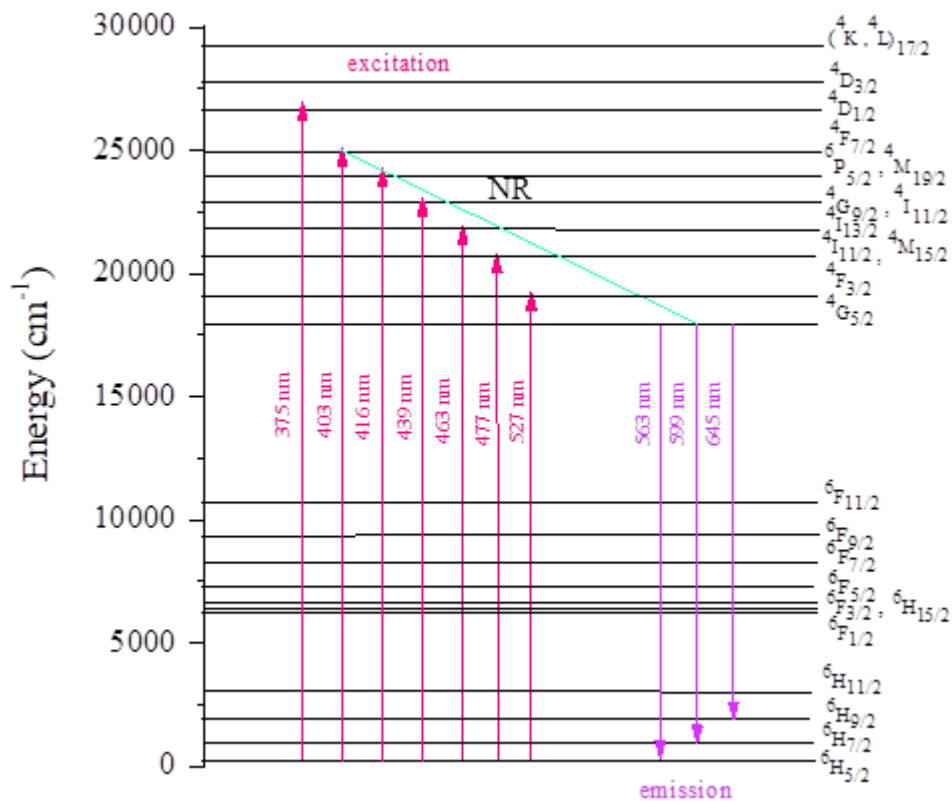


FIGURE 4. Energy level diagram of Sm^{3+} doped borate glasses.

Judd-Ofelt Analysis

TABLE 1 shows the results of the calculation of the oscillator strength both experimental ($f_{exp} \times 10^{-6}$) and calculated ($f_{cal} \times 10^{-6}$) as well as the results of the calculation of the root mean square deviation (δ_{rms}) of Sm^{3+} ion doped borate glass.

TABLE 1. The value of oscillator strength ($f \times 10^{-6}$) was experimental and calculated for BZLNPSm 0.05; BZLNPSm 0.1; BZLNPSm 0.5; BZLNPSm 1.0; BZLNPSm 2.0; BZLNPSm 4.0; glasses.

Transition	λ_{abs} (nm)	E_{exp} (cm^{-1})	BZLNPSm 0.05		BZLNPSm 0.10		BZLNPSm 0.50		BZLNPSm 1.00		BZLNPSm 2.00		BZLNPSm 4.00	
			f_{exp}	f_{cal}										
${}^6H_{5/2} \rightarrow$														
${}^4D_{7/2}$	341	29325.5	3.21	2.73	2.82	2.66	3.74	3.32	2.99	2.83	2.05	2.59	3.19	2.36
${}^4D_{3/2}$	362	27624.3	1.05	1.03	1.11	1.10	3.06	3.01	2.75	2.72	1.61	2.52	2.69	2.66
${}^4D_{1/2}$	377	26525.2	0.00	0.00	1.02	0.00	0.75	0.00	0.83	0.00	0.91	0.00	0.77	0.00
							4		3		2		2	
${}^4F_{7/2}$	403	24813.9	0.00	0.06	0.44	0.06	0.65	1.58	0.96	0.14	1.38	0.13	1.07	0.13
${}^4G_{9/2}$	439	22779.0	0.70	0.19	0.37	0.19	0.27	0.30	0.24	0.25	0.21	0.23	0.31	0.22
${}^4I_{11/2}$	475	21052.6	0.61	0.56	0.65	0.55	0.58	0.67	0.62	0.57	0.53	0.53	0.66	0.48
${}^6F_{11/2}$	947	10559.7	1.06	1.35	0.90	1.32	2.45	1.64	2.17	1.40	1.36	1.28	1.21	1.16
${}^6F_{9/2}$	1080	9259.3	8.05	8.08	7.37	7.90	10.1	10.1	8.73	8.71	8.09	7.99	7.54	7.35
							0	9						
${}^6F_{7/2}$	1234	8103.7	10.5	10.3	10.8	10.2	15.6	15.4	13.4	13.4	12.3	12.2	11.7	11.7
			8	6	4	5	1	3	7	0	6	3	0	5
${}^6F_{5/2}$	1376	7267.4	3.00	3.08	3.17	3.27	9.18	9.30	8.06	8.32	7.18	7.58	7.64	8.06
${}^6F_{3/2}$	1476	6775.1	1.40	1.43	1.21	1.47	5.62	5.53	5.05	4.62	4.63	3.88	4.96	4.13
${}^6H_{15/2}$	1520	6578.9	0.46	0.07	0.37	0.07	0.10	0.08	0.09	0.07	0.06	0.07	0.07	0.06
${}^6F_{1/2}$	1583	6317.1	0.11	0.08	0.20	0.01	1.89	1.93	1.01	1.27	0.24	0.69	0.21	0.73
${}^6H_{13/2}$	2022	4945.6	0.03	0.81	0.04	0.79	0.21	0.98	0.18	0.83	0.21	0.77	0.24	0.70
δ_{rms}			0.316		0.448		0.405		0.443		0.584		0.507	

The results showed that the ${}^6H_{5/2} \rightarrow {}^6F_{7/2}$ transition at a wavelength of 1234 nm displayed the highest magnitudes f_{exp} and f_{cal} , which are called hypersensitive transitions [6]. Relatively small rms deviation indicates a good match between the experimental and calculated spectral intensities which are shown at a value of 0.316 [6, 24].

TABLE 2. Judd-Ofelt parameter values ($\times 10^{-20} cm^2$) and quality factors for Sm^{3+} Borate glass.

Glass	Ω_2	Ω_4	Ω_6	$\chi(\Omega_4/\Omega_6)$	Trend	Reference
BZLNPSm 0.05	0.25	5.80	9.64	0.62	$\Omega_6 > \Omega_4 > \Omega_2$	Present work
BZLNPSm 0.10	0.03	6.12	9.31	0.66	$\Omega_6 > \Omega_4 > \Omega_2$	Present work
BZLNPSm 0.50	6.0	16.4	11.3	1.45	$\Omega_4 > \Omega_6 > \Omega_2$	Present work
BZLNPSm 1.00	3.98	14.95	9.67	1.55	$\Omega_4 > \Omega_6 > \Omega_2$	Present work
BZLNPSm 2.00	2.16	13.67	8.78	1.55	$\Omega_4 > \Omega_6 > \Omega_2$	Present work
BZLNPSm 4.00	2.25	14.60	7.97	1.83	$\Omega_4 > \Omega_6 > \Omega_2$	Present work
NNS01	0.33	5.45	0.55	0.98	$\Omega_2 > \Omega_4 > \Omega_6$	[18]
PNZSm0.5	4.46	6.79	10.91	0.62	$\Omega_6 > \Omega_4 > \Omega_2$	[25]
PZSMS-Ag0.2	12.69	5.29	4.07	1.30	$\Omega_2 > \Omega_4 > \Omega_6$	[26]
PKACaLFSm10	5.87	9.75	4.82	1.66	$\Omega_4 > \Omega_2 > \Omega_6$	[27]
SLfSfASm1.0	2.73	7.49	3.01	3.84	$\Omega_4 > \Omega_6 > \Omega_2$	[28]
TSWS2	0.12	3.36	2.65	1.26	$\Omega_4 > \Omega_6 > \Omega_2$	[29]
TWSm10	2.01	4.38	1.56	2.81	$\Omega_4 > \Omega_2 > \Omega_6$	[30]
TeWNaSm	0.27	3.36	3.30	1.02	$\Omega_4 > \Omega_6 > \Omega_2$	[31]

TABLE 3. Radiative properties, such as emission peak wavelength (λ_p), effective bandwidth ($\Delta\lambda_{\text{eff}}$), emission cross-section ($\sigma_e(\lambda_p) \times 10^{-20}$), branching ratio (β_R) and radiative transition probability (A_R), of various Sm^{3+} -doped borate glasses.

Glass	Transition $^4G_{3/2} \rightarrow$	λ_p (nm)	$\Delta\lambda_{\text{eff}}$ (nm)	$\sigma_e(\lambda_p)$ (cm^2)	β_{exp} (%)	β_{cal} (%)	A_R (s^{-1})
BZLNPSm 0.05	$^6H_{5/2}$	563	9.220	0.013	0.134	0.047	23.46
	$^6H_{7/2}$	599	14.282	0.128	0.622	0.762	278.26
	$^6H_{9/2}$	645	13.450	0.062	0.244	0.191	94.53
BZLNPSm 0.10	$^6H_{5/2}$	562	12.764	0.010	0.151	0.048	24.49
	$^6H_{7/2}$	598	15.948	0.117	0.576	0.758	284.66
	$^6H_{9/2}$	644	17.663	0.050	0.273	0.195	99.39
BZLNPSm 0.50	$^6H_{5/2}$	563	11.243	0.020	0.144	0.040	44.63
	$^6H_{7/2}$	599	14.976	0.227	0.600	0.667	516.77
	$^6H_{9/2}$	645	15.896	0.185	0.255	0.294	332.03
BZLNPSm 1.00	$^6H_{5/2}$	562	12.294	0.017	0.149	0.042	40.33
	$^6H_{7/2}$	598	15.596	0.191	0.581	0.680	454.01
	$^6H_{9/2}$	644	17.126	0.138	0.270	0.278	267.54
BZLNPSm 2.00	$^6H_{5/2}$	562	11.803	0.016	0.149	0.044	37.73
	$^6H_{7/2}$	598	15.275	0.180	0.608	0.697	420.46
	$^6H_{9/2}$	644	14.091	0.139	0.242	0.259	222.22
BZLNPSm 4.00	$^6H_{5/2}$	563	5.078	0.039	0.094	0.045	38.78
	$^6H_{7/2}$	599	11.719	0.235	0.652	0.690	417.36
	$^6H_{9/2}$	645	9.115	0.224	0.254	0.266	230.32

In general, the covalence and asymmetry of the ligand field which is precisely around the Sm^{3+} ion site can affect the Ω_2 parameter, while the parameter values of Ω_4 and Ω_6 can be related to the viscosity and stiffness of the host medium, both of which are included in the bulk properties [11, 24]. It can be seen in TABLE 2 that the high value of Ω_6 and Ω_4 parameters indicates that the viscosity and stiffness of the host medium are getting higher in the glass, this is because more BO_4 units are observed in the glass [25-27]. The spectroscopic quality factor $\chi = (\Omega_4 / \Omega_6)$ describes the quality of the glass. TABLE 2 has summarized the calculation of the spectroscopic quality factor for borate glass doped Sm^{3+} . Based on this factor, it was found that BZLNPSm 0.5 glass looks like a better optical glass [25].

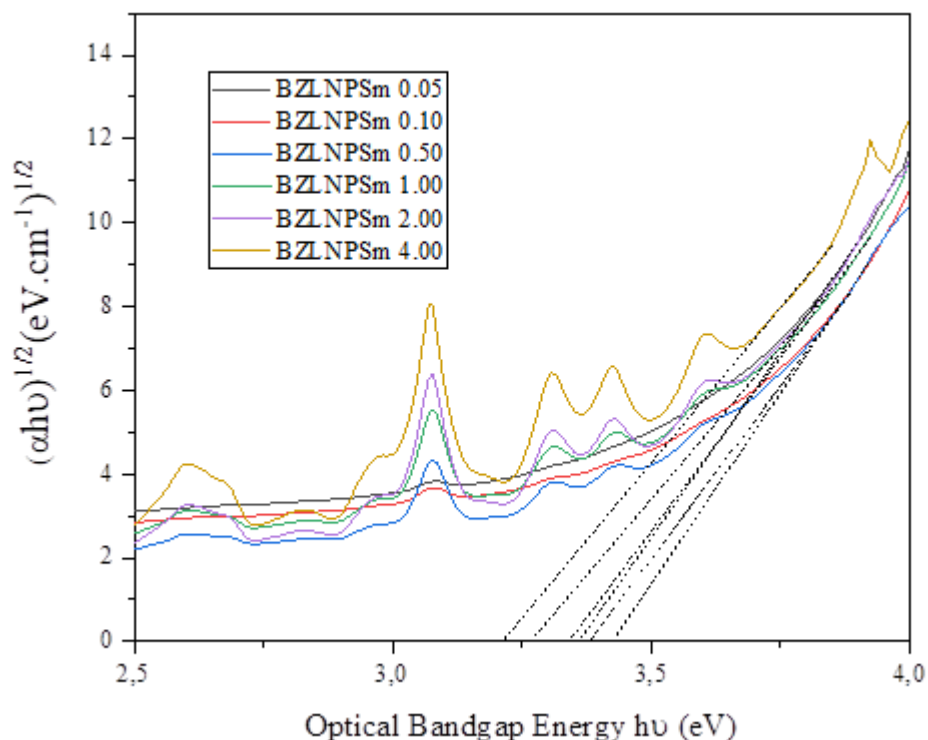
The radiative properties that are emission peak wavelength (λ_p), effective bandwidth ($\Delta\lambda_{\text{eff}}$), spontaneous emission transition probability (A_R), stimulated emission cross section ($\sigma(\lambda_p)$), and the branching ratio (B_R) both the experimental (exp) and calculation (cal) on Sm^{3+} doped borate glass are summarized in TABLE 3. The non-radiation transition that occurs between Sm^{3+} ions causes a difference in the values of β_{exp} and β_{cal} [35]. It can be observed in TABLE 3 that the A_R and $\sigma(\lambda_p)$ values in the $^4G_{5/2}$ to $^6H_{7/2}$ transition have a higher value than the other transitions, where the β_R value has a value of more than 0.5 indicates that the Sm^{3+} doped borate glass has a high potential as a laser amplifying medium for emissions around 599 nm due to its high amplifying power, low laser threshold, and high gain laser applications in the reddish-orange region of the spectrum, which is useful in underwater communications and medical diagnostic applications [6, 35, 37].

TABLE 4. The radiative properties for transition ${}^4G_{3/2} \rightarrow {}^4H_{7/2}$ of various Sm^{3+} -doped sodium borate glasses compared with other Sm-doped glass.

Label Glasses	$A_R (s^{-1})$	$\sigma_e (\lambda_p)$ (cm^2)	β_{exp} (%)	β_{cal} (%)	Reference
BZLNPSm 0.05	278.26	0.13	0.622	0.762	Present work
BZLNPSm 0.10	284.66	0.12	0.576	0.758	Present work
BZLNPSm 0.50	516.77	0.23	0.600	0.667	Present work
BZLNPSm 1.00	454.01	0.19	0.581	0.680	Present work
BZLNPSm 2.00	420.46	0.18	0.608	0.697	Present work
BZLNPSm 4.00	417.36	0.24	0.652	0.690	Present work
SLfSfASm1.0	185.00	0.10	0.46	0.47	[28]
TeWNaSm	399.51	0.21	0.47	0.51	[31]
$\text{TeO}_2\text{eZnF}_2\text{ePbOeNb}_2\text{O}_5\text{eSm}_2\text{O}_3$	259.00	0.11	0.48	0.48	[32]
PKANbSm10	271	0.12	0.423	0.366	[33]
Sm4 BI	565.76	0.31	0.52	0.55	[34]
Glass A	228.4	0.13	0.57	0.34	[35]

Bandgap Energy

The function of the bandgap is very important, namely to analyze the fundamentals of the absorption edge of crystalline and non-crystalline materials [36-37]. To determine the properties of solid materials, there are two types of transitions that are generally used, namely direct transitions and indirect transitions [36]. In this study, the Sm^{3+} doped borate glass bandgap was calculated and summarized in FIGURE 5, FIGURE 6 and TABLE 5.

**FIGURE 5.** Indirect Bandgap

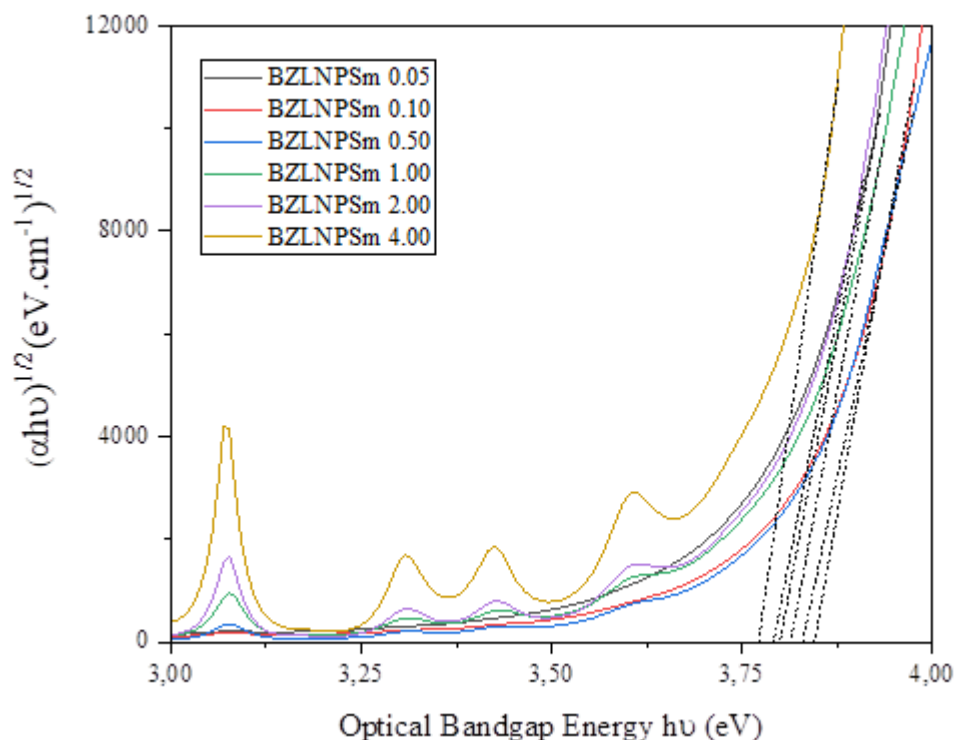


FIGURE 6. Direct Bandgap

The energy of the optical bandgap is in the range 3.85-3.77 eV for direct transitions and 3.42 - 4.22 eV for indirect transitions. From these data it can be concluded that the optical bandgap depends on the composition of Sm^{3+} . Based on TABLE 5, it can be seen that at the Sm^{3+} ion concentration, namely BZLNPSm 0.1 to BZLNPSm 4.0, the direct and indirect bandgap values were found to decrease with the increase in Sm_2O_3 . Due to the formation of more NBO (non-bridging oxygen) in the host matrix by the structural rearrangement of the BO_3 units into BO_4 units causes the optical absorption edge wavelength of the glasses is shifted to the lower energy side of the electromagnetic spectrum. NBO binds to less excited electrons than the bridging oxygen [19].

TABLE 5. Optical Bandgap of Sm^{3+} doped Sodium Borate glass system a) Indirect and b) Direct

No	Glass Initial	Indirect Bandgap	Direct Bandgap	Reference
1.	BZLNPSm 0.05	3.36	3.80	Present work
2.	BZLNPSm 0.10	3.42	3.85	Present work
3.	BZLNPSm 0.50	3.39	3.83	Present work
4.	BZLNPSm 1.00	3.34	3.81	Present work
5.	BZLNPSm 2.00	3.26	3.79	Present work
6.	BZLNPSm 4.00	3.22	3.77	Present work
7.	NPABSSm5	3.94	4.02	[19]
8.	PZSMS-Ag0.5	3.74	4.13	[26]
9.	0.05 LBTPS	2.99	3.16	[36]
10.	Sm 0.4	3.11	3.21	[37]
11.	1.0 CSm	3.11	3.12	[38]
12.	Zinc-phosphate glasses 5%	3.96	3.96	[39]

Radiative Lifetime

FIGURE 7 shows the decay time curve. The decay times obtained were 3.42, 3.99, 3.98, 2.96, 1.67, 1.48 ms for 0.05, 0.1, 0.5, 1.00, 2.00 and 4.00 mol% of Sm_2O_3 doped in borate glass, respectively. The lifetime decreases when the Sm_2O_3 concentration increases due to an increase in the energy transfer process of the Sm^{3+} ion [11, 40].

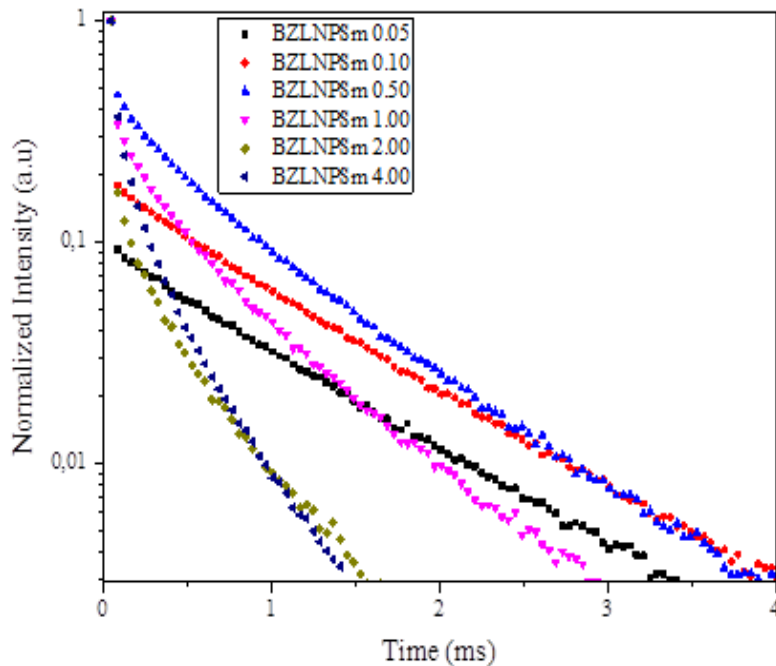


FIGURE 7. Lifetime of Sm^{3+} Doped Glasses

CIE Chromaticity Diagram

The x, y color coordinates of the light emission, carried out with the CIE 1931 chromaticity diagram, found that the x, y coordinates were (0.5939, 0.4053); (0.5921, 0.4072); (0.5954, 0.4039); (0.5926, 0.4066); (0.5921, 0.4071); (0.5945, 0.4047) corresponding to 0.05, 0.1, 0.5, 1.00, 2.00 and 4.00 mol% of Sm_2O_3 doped in borate glasses, respectively.

in particular as a laser amplifying medium for emissions around 599 nm due to its high amplifying power, low laser threshold, and high gain laser applications in the orange region of the spectrum.

ACKNOWLEDGEMENT

The authors would like to thank the Directorate of Research and Community Services (DRPM) for the funding grants with contract No. 130/SP2H/LT/DRPM/2021.

REFERENCES

- [1] K. Shaaban *et al.*, "Spectroscopic properties and Judd-Ofelt analysis of Dy³⁺ ions in molybdenum borosilicate glasses," *J. Lumin*, vol. 196, pp. 477-484, 2018.
- [2] J. Rajagukguk *et al.*, "Structural and optical characteristics of Eu³⁺ ions in sodium-lead-zinc-lithium-borate glass system," *J. Mol. Struct*, vol. 1121, pp. 180-187, 2016.
- [3] N. Chanthima *et al.*, "Photoluminescence study of barium borophosphate glasses doped with Sm³⁺ ions," *Mat.Today Proceed*, vol. 5, no. 7, pp. 15049-15053, 2018.
- [4] J. Rajagukguk *et al.*, "Structural, spectroscopic and optical gain of Nd³⁺ doped fluorophosphate glasses for solid state laser application," *Journal of Luminescence*, vol. 216, p. 116738, 2019.
- [5] N. Sangwaranatee *et al.*, "Effect of alkali oxide on optical and luminescence properties of Sm³⁺ doped aluminium phosphate glasses," *Materials Today: Proceedings*, vol. 5, no. 6, pp. 13891-13895, 2018.
- [6] N. Chanthima *et al.*, "Luminescence properties and Judd-Ofelt analysis of Sm³⁺ doped lithium aluminium phosphate glasses," *Materials Today: Proceedings*, vol. 5, no. 7, pp. 15034-15039, 2018.
- [7] Prabhu *et al.*, "Physical, structural and optical properties of Sm³⁺ doped lithium zinc alumino borate glasses," *Journal of Non-Crystalline Solids*, vol. 515, pp. 116-124, 2019.
- [8] M. Shoaib *et al.*, "Comparative study of Sm³⁺ ions doped phosphate based oxide and oxy-fluoride glasses for solid state lighting applications," *Journal of Rare Earths*, vol. 37, no. 4, pp. 374-382, 2019.
- [9] J. Rajagukguk *et al.*, "Preparation and Structural Characterization of Dy³⁺-Doped PBiNaGd Glass," *Integrated Ferroelectrics*, vol. 214, no. 1, pp. 151-157, 2021.
- [10] Prabhu *et al.*, "Investigations on the physical, structural, optical and photoluminescence behavior of Er³⁺ ions in lithium zinc fluoroborate glass system," *Journal of Infrared Physics and Technology*, vol. 98, pp. 7-15, 2019.
- [11] J. Rajagukguk *et al.*, "Emission cross section and optical gain of 1.06 μ m laser Nd³⁺ doped borate glasses," *Materials Today: Proceedings*, vol. 5, no. 7, pp. 14998-15003, 2018.
- [12] N. Sdiri *et al.*, "Spectroscopic properties of Er³⁺ and Yb³⁺ doped phosphate-borate glasses," *Journal of Molecular Structure*, vol. 1010, pp. 85-90, 2012.
- [13] S. Selvi, K. Marimuthu and G. Muralidharan, "Effect of PbO on the B₂O₃-TeO₂-P₂O₅-BaO-CdO-Sm₂O₃ glasses - Structural and optical investigations," *Journal of Non-Crystalline Solids*, vol. 461, pp. 35-46, 2017.

- [14] N. Sdiri, H. Elhouichet and M. Ferid, "Effects of substituting P₂O₅ for B₂O₃ on the thermal and optical properties of sodium borophosphate glasses doped with Er," *Journal of Non-Crystalline Solids*, vol. 389, pp. 38-45, 2014, <https://doi.org/10.1016/j.jnoncrysol.2014.01.031>
- [15] G. Lakshminarayana *et al.*, "Effect of alkali/mixed alkali metal ions on the thermal and spectral characteristics of Dy³⁺:B₂O₃-PbO-Al₂O₃-ZnO glasses," *Journal of Non-Crystalline Solids*, vol. 481, pp. 191-201, 2018.
- [16] A. Balakrishna, D. Rajesh and Y. C. Ratnakaram, "Structural and optical properties of Nd³⁺ in lithium fluoro-borate glass with relevant modifier oxides," *Optical Materials*, vol. 35, no. 12, pp. 2670-2676, 2013.
- [17] J. Rajagukguk *et al.*, "Structural and optical properties of Nd³⁺ doped Na₂O-PbO-ZnO-Li₂O-B₂O₃ glasses system," *Key Engineering Materials*, vol. 675, pp. 424-429, 2016.
- [18] I. Jlassi, S. Mnasri and H. Elhouichet, "Concentration dependent spectroscopic behavior of Sm³⁺-doped sodium fluoro-phosphates glasses for orange and reddish-orange light emitting applications," *Journal of Luminescence*, vol. 199, pp. 516-527, 2018.
- [19] J. Rajagukguk *et al.*, "Physical and Structural Properties of Sm³⁺ Doped Phosphate Glasses," *Integrated Ferroelectrics*, vol. 214, no. 1, pp. 143-150, 2021.
- [20] Y. Tariwong *et al.*, "Optical properties and Judd-Ofelt analysis of Dy³⁺ doped MgO-BaO-P₂O₅ glass systems," *Proceedings - 2015 4th International Conference on Instrumentation, Communications, Information Technology and Biomedical Engineering*, ICICI-BME, pp. 264-267, 2015.
- [21] V. Rajeswara Rao and C. K. Jayasankar, "Spectroscopic investigations on multi-channel visible and NIR emission of Sm³⁺-doped alkali-alkaline earth fluoro phosphate glasses," *Optical Materials*, vol. 91, pp. 7-16, 2019.
- [22] J. Rajagukguk *et al.*, "Investigation of Sm³⁺-doped PBNaG glasses for orange LED applications," *Journal of the Korean Physical Society*, vol. 78, no. 3, pp. 177-181, 2021.
- [23] M. Yang *et al.*, "Temperature-dependent and threshold behavior of Sm³⁺ ions on fluorescence properties of lithium niobate single crystals," *Materials*, vol. 11, no. 10, pp. 1-12, 2018.
- [24] I. I. Kindrat, B. V. Padlyak and R. Lisiecki, "Judd-Ofelt analysis and radiative properties of the Sm³⁺ centres in Li₂B₄O₇, CaB₄O₇, and LiCaBO₃ glasses," *Optical Materials*, vol. 49, pp. 241-248, 2015.
- [25] H. Largot *et al.*, "Spectroscopic investigations of Sm³⁺-doped phosphate glasses: Judd-Ofelt analysis," *Physica B: Condensed Matter*, vol. 552, pp. 184-189, 2019.
- [26] F. Ahmadi, R. Hussin and S. K. Ghoshal, "Spectroscopic attributes of Sm³⁺ doped magnesium zinc sulfophosphate glass: Effects of silver nanoparticles inclusion," *Optical Materials*, vol. 73, pp. 268-276, 2017.
- [27] K. Kiran Kumar and C. K. Jayasankar, "Visible luminescence of Sm³⁺:K-Ca-Li fluorophosphate glasses," *Journal of Molecular Structure*, vol. 1074, pp. 496-502, 2014.
- [28] C. S. Dwaraka Viswanath and C. K. Jayasankar, "Photoluminescence, γ -irradiation and X-ray induced luminescence studies of Sm³⁺-doped oxyfluorosilicate glasses and glass-ceramics," *Ceramics International*, vol. 44, no. 6, pp. 6104-6114, 2018.

- [29] V. H. Rao *et al.*, “Luminescence properties of Sm³⁺ ions doped heavy metal oxide tellurite-tungstate-antimonate glasses,” *Ceramics International*, vol. 43, no. 18, pp. 16467-16473, 2017.
- [30] G. Venkataiah *et al.*, Concentration dependent luminescence properties of Sm³⁺-ions in tellurite-tungsten-zirconium glasses,” *Optical Materials*, vol. 40, pp. 26-35, 2015.
- [31] C. B. A. Devi *et al.*, “Spectroscopic studies and lasing potentialities of Sm³⁺ ions doped single alkali and mixed alkali fluoro tungstentellurite glasses,” *Optics and Laser Technology*, vol. 111, pp. 176-183, 2019.
- [32] B. Klimesz, R. Lisiecki and W. Ryba Romanowski, “Sm³⁺-doped oxyfluorotellurite glasses - spectroscopic, luminescence and temperature sensor properties,” *Journal of Alloys and Compounds*, vol. 788, pp. 658-665, 2019.
- [33] T. Srihari and C. K. Jayasankar, “Spectral investigations of Sm³⁺-doped niobium phosphate glasses,” *Optical Materials*, vol. 66, pp. 35-42, 2017.
- [34] A. Wagh *et al.*, “The effect of 1.25 MeV γ rays on Sm³⁺ doped lead fluoroborate glasses for reddish orange laser and radiation shielding applications,” *Journal of Luminescence*, vol. 199, pp. 87-108, 2018.
- [35] N. Deopa *et al.*, “Photoluminescence investigations on Sm³⁺ ions doped borate glasses for tricolor w-LEDs and lasers,” *Materials Research Bulletin*, vol. 100, pp. 206-212, 2018
- [36] S. Selvi, K. Marimuthu and G. Muralidharan, “Structural and luminescence behavior of Sm³⁺ ions doped lead boro-telluro-phosphate glasses,” *Journal of Luminescence*, vol. 159, pp. 207-218, 2015.
- [37] J. Rajagukguk, B. Sinaga and J. Kaewkhao, “Structural and spectroscopic properties of Er³⁺ doped sodium lithium borate glasses,” *Spectrochimica Acta Part A: Molecular and Biomolecular Spectroscopy*, vol. 223, p. 117342, 2019.
- [38] T. Sambasiva Rao *et al.*, “Energy transfer (Ce³⁺ \rightarrow Sm³⁺) influence on PL emission of Ce³⁺ /Sm³⁺ co-doped barium gallium borosilicate glasses,” *Physica B: Condensed Matter*, vol. 559, pp. 8-16, 2019.
- [39] M. Seshadri *et al.*, “Effect of ZnO on spectroscopic properties of Sm³⁺ doped zinc phosphate glasses,” *Physica B: Condensed Matter*, vol. 459, pp. 79-87, 2015.
- [40] S. Damodaraiah, V. Reddy Prasad and Y. C. Ratnakaram, “Structural and luminescence properties of Sm³⁺-doped bismuth phosphate glass for orange-red photonic applications,” *Luminescence*, vol. 33, no. 3, pp. 594-603, 2018.